Hindawi Publishing Corporation
Journal of Combustion
Volume 2011, Article ID 678719, 8 pages
doi:10.1155/2011/678719

Research Article

Sensitivity and Effect of Ignition Timing on the Performance of a Spark Ignition Engine: An Experimental and Modeling Study

A. H. Kakaee, M. H. Shojaeefard, and J. Zareei

Department of Automotive Engineering, Iran University of Science and Technology, Tehran, Iran

Correspondence should be addressed to A. H. Kakaee, kakaee_ah@iust.ac.ir

Received 24 December 2010; Accepted 12 January 2011

Academic Editor: Xingcai Lu

The performance of a spark ignition engine is investigated under different values of ignition advance. A two-zone burnt/unburned model with the fuel burning rate described by a Wiebe function is used for modeling in-cylinder combustion, and then experiments are carried out to validate the calculated data. By varying the ignition timing, the results of some characteristics such as power, torque, thermal efficiency, pressure, and heat release are obtained and compared. The results show that optimal power and torque are achieved at 31°CA before top dead center, and performance is decreased if this ignition timing is changed. It is also shown that the maximum thermal efficiency is accomplished when peak pressure occurs between 5 and 15°CA after top dead center.

1. Introduction

Since the advent of Otto's first four-stroke engine, the development of the spark ignition (SI) engine has achieved a high level of success. In the early years, increasing engine power and engine working reliability was the principal aim for engine designers. In recent years, however, ignition timing has brought increased attention to the development of advanced SI engines for maximizing performance [1, 2].

Additionally, optimization of the engine design and operating variables requires extensive engine testing. Therefore, engine modeling codes are generally preferred for assessing initial designs. Computer models of engine processes are useful tools for analysis and optimization of engine performance and allow exploration of many engine design alternatives in an inexpensive method. For any given engine design and operating condition, in-cylinder pressure-time and temperature-time traces can be predicted. Furthermore, parameters such as ignition timing, exhaust gas recirculation ratio, and equivalence ratio can be optimized for the best performance. Since the burned and unburned zone thermodynamic states can be calculated, the knock limits and emissions can be estimated.

Moreover, modeling the performance of internal combustion engines has been a continuous attempt over the years, and many models have been developed to predict engine performance parameters. Some of the models employ assumptions to simplify the flow and combustion processes [3–5]. Others use multidimensional reactive flow codes for elaborate modeling of engine flow and combustion processes, which are very sophisticated [6–8]. Accurate prediction of the performance parameters and exhaust emissions depends on the flow dynamics in the intake manifold, the heat transfer, and the ignition timing. It is feasible to model all these processes with multi-dimensional flow codes coupled to detailed chemical kinetic mechanisms with some support of experiment data. The KIVA-CHEMKIN combination is an example for the detailed modeling of flow and combustion processes in internal combustion engines [9]. However, multidimensional modeling of all these processes from the intake manifold to the exhaust manifold takes extensive computation time and very powerful computers [10–12].

Therefore, a reasonable choice sounds to be a two-zone combustion model, which includes the effects of changes in engine design and operation on the details of the combustion process through a phenomenological model where the geometric details are fairly well approximated by detailed modeling of the different mechanisms involved [13–15]. This is going to have the advantages of relative simplicity and very reasonable computer time cost.

Table 1: Engine specifications.

Engine type	TU3A
Number of strokes	4
Number of cylinders	4
Cylinder diameter (mm)	75
Stroke (mm)	77
Compression ratio	10.5 : 1
Maximum power (kW)	50
Maximum torque (NM)	160
Maximum speed (rpm)	6500
Displacement (cc)	1360
Fuel	97-octane

The performance of spark ignition engines is a function of many factors. One of the most important ones is ignition timing. Chan and Zhu worked on modeling of in-cylinder thermodynamics under high values of ignition retard, in particular the effect of spark retard on cylinder pressure distribution. In-cylinder gas temperature and trapped mass under varying spark timing conditions were also calculated [1]. Soylu and Van Gerpen developed a two-zone thermodynamic model to investigate the effects of ignition timing, fuel composition, and equivalence ratio on the burning rate and cylinder pressure for a natural gas engine. Burning rate analysis was carried out to determine the flame initiation period and the flame propagation period at different engine operating conditions [2].

The objective of the present work is to examine the effect of the ignition timing on the performance of an SI engine. For achieving this goal, at a speed of 3400 rpm, the ignition timing has been changed in the range of 10°CA ATDC to 41°CA BTDC, and the performance characteristics such as power, torque, thermal efficiency, pressure, and heat release are obtained and compared.

2. Test Engine

Facilities to monitor and control engine variables such as engine speed, engine load, water and lube oil temperatures, and fuel and air flows, are installed on a fully automated test bed, four-cylinder, water cooled, naturally aspirated, experimental standard SI engine, located at the Iran Khodro Company Laboratory. The first set of performance data was taken varying timing angle, the intake manifold pressure was 100 Kpa, and equivalence was held at unity. The specifications of the test engine are given in Table 1.

The engine is mounted on a fully automated test bed and coupled to a Schenck W130 eddy current dynamometer, having load absorbing and motoring capabilities. There is one electric sensor for speed and one for load, with these signals fed to indicators on the control panel and to the controller. Via knobs on the control panel, the operator can set the dynamometer to control speed or load. There is also a capability of setting the ignition timing from a switch on the control panel.

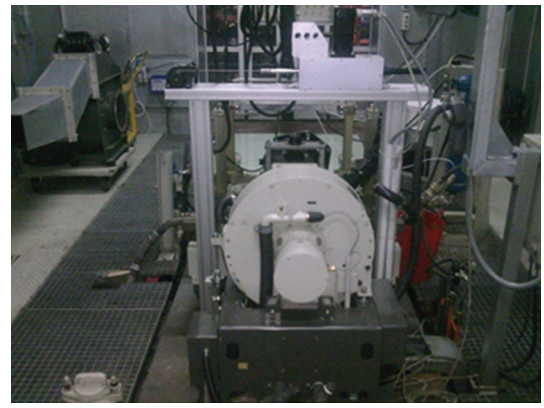

Figure 1: The photo of the engine tested.

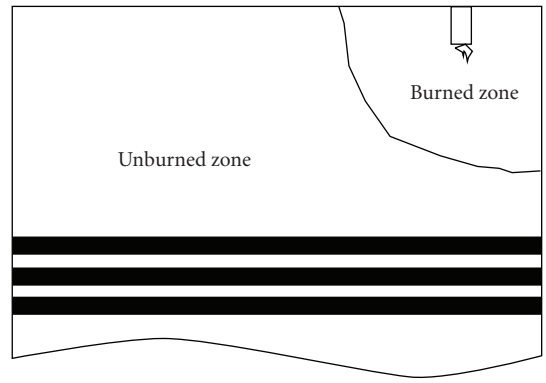

Figure 2: Burned and unburned zones of combustion chamber.

The coolant and lube oil circulation is achieved by electrically driven pumps, with the temperature controlled by water-fed heat exchangers. Heaters are used to maintain the oil and coolant temperatures during warm-up and light load conditions. Figure 1 is the photo of the engine tested.

3. Description of the Model

A zero-dimensional thermodynamic cycle model with two-zone burnt/unburned combustion model, mainly based on Ferguson's and Krikpatrick work [16], was developed to predict the cylinder pressure, work done, heat release, enthalpy of exhaust gas, and so forth. The zero-dimensional model is based on the first law of thermodynamics in which an empirical relationship between the fuel burning rate and crank angle position is established. Figure 2 shows the burned and unburned zones, which are presumed to be separated by an infinitesimally thin flame front. The burned zone consists of the equilibrium products of combustion, and both zones are assumed to be at the same pressure at any CA degree.

The region in the combustion chamber is treated as a control volume. The governing equations include the mass and energy conservation equations and equations of state. These equations, with crank angle as the independent

variable, form the building block of this thermodynamic model.

4. Mathematical Formulation of the Present Model

4.1. Mass and Energy Balances. For a control volume enclosing the fuel-air mixture, the rate of change of total mass of an open system is equal to the sum of mass flowing into and out of the system [1]:

$$\dot{m} = \sum_j \dot{m}_j. \tag{1}$$

Applying the first law of thermodynamics to an open thermodynamic system, the energy equation is

$$\dot{E} = \dot{Q} - \dot{W} + \sum_j \dot{m}_j h_j. \tag{2}$$

Prescribing the conservation of mass and energy equations as functions of crank angle, (1) and (2) become

$$\frac{dm}{d\theta} = \sum_j \frac{dm_j}{d\theta}, \tag{3}$$

$$\frac{d(mu)}{d\theta} = \frac{dQ}{d\theta} - p\frac{dV}{d\theta} + \sum_j h_j \frac{d\dot{m}}{d\theta}. \tag{4}$$

The latter neglects the changes of kinetic energy and potential energy in the control volume.

4.2. Thermal Properties. In a two-zone burnt/unburned model, the unburned mixture and burnt mixture zones are each treated as separate open systems. Hence, the specific internal energy and volume are given by

$$u = \frac{U}{m} = xu_b + (1-x)u_u, \tag{5}$$

$$v = \frac{V}{m} = xv_b + (1-x)v_u. \tag{6}$$

Assuming that the pressures of burnt and unburned gases are equal, v_b and v_u are functions of T_b, T_u, and p. Hence,

$$\begin{aligned} \frac{dv_b}{d\theta} &= \frac{dv_b}{dT_b}\frac{dT_b}{d\theta} + \frac{\partial v_b}{\partial p}\frac{dp}{d\theta}, \\ \frac{dv_u}{d\theta} &= \frac{\partial v_u}{\partial T_u}\frac{dT_u}{d\theta} + \frac{\partial v_u}{\partial p}\frac{dp}{d\theta}. \end{aligned} \tag{7}$$

The thermodynamic properties of a complex chemical equilibrium composition existing in any fuel-air reaction are obtained using the method proposed by Olikara and Borman [17] which is an equilibrium constant-based method for solving chemical equilibrium compositions, specific heats, internal energies, enthalpies, entropies, and other partial derivatives useful in thermodynamic analysis.

By substituting logarithmic derivatives obtained from Olikara and Borman's method, (7) can be rewritten as

$$\begin{aligned} \frac{dv_b}{d\theta} &= \frac{v_b}{T_b}\frac{\partial \ln v_b}{\partial \ln T_b}\frac{dT_b}{d\theta} + \frac{v_u}{p}\frac{\partial \ln v_b}{\partial \ln p}\frac{dp}{d\theta}, \\ \frac{dv_u}{d\theta} &= \frac{v_u}{T_u}\frac{d \ln v_u}{d \ln T_u}\frac{dT_u}{d\theta} + \frac{v_b}{p}\frac{\partial \ln v_u}{\partial \ln p}\frac{dp}{d\theta}. \end{aligned} \tag{8}$$

Likewise, the internal energies of both the burnt and unburned gases with the same pressure condition are

$$\begin{aligned} \frac{du_b}{d\theta} &= \frac{\partial u_b}{\partial T_b}\frac{dT_b}{d\theta} + \frac{\partial u_b}{\partial p}\frac{dp}{d\theta}, \\ \frac{du_u}{d\theta} &= \frac{\partial u_u}{\partial T_u}\frac{dT_u}{d\theta} + \frac{\partial u_u}{\partial p}\frac{dp}{d\theta}. \end{aligned} \tag{9}$$

Variation of mass due to the crank angle is given in the next equation. According to the mass conservation equation and mass loss which is caused by gas leakage through the rings, the mass ratio due to crank angle is

$$\frac{dm}{d\theta} = \frac{-C_m}{\omega}, \tag{10}$$

where ω is the rotational speed of engine and the constant, c, is related to the engine ring's design. Equation (9) can be rewritten to include the logarithmic terms (4) as

$$\begin{aligned} \frac{du_b}{d\theta} &= \left(c_{pb} - \frac{pv_b}{T_b}\frac{\partial \ln v_b}{\partial \ln T_b}\right)\frac{dT_b}{d\theta} \\ &\quad - v_b\left(\frac{\partial \ln v_b}{\partial \ln T_b} + \frac{\partial \ln v_b}{\partial \ln p}\right)\frac{dp}{d\theta}, \\ \frac{du_u}{d\theta} &= \left(c_{pu} - \frac{pv_u}{T_u}\frac{\partial \ln v_u}{\partial \ln T_u}\right)\frac{dT_u}{d\theta} \\ &\quad - v_u\left(\frac{\partial \ln v_u}{\partial \ln T_u} + \frac{\partial \ln v_u}{\partial \ln p}\right)\frac{dp}{d\theta}. \end{aligned} \tag{11}$$

4.3. Fuel Burning Rate Correlation. The fuel burning rate in the SI engine is normally modelled by the Wiebe function [18]. The burnt mass fraction is given by

$$x(\theta) = 1 - \exp\left[-a\left(\frac{\theta - \theta_{ig}}{\theta_b}\right)^n\right]. \tag{12}$$

Values of $a = 5$ and $n = 3$ have been reported to fit with experimental data.

4.4. Heat Transfer from Gases to Cylinder Wall. Heat transfer into a thermodynamic system is expressed in terms of the heat loss:

$$\frac{dQ}{d\theta} = \frac{-\dot{Q}_l}{\omega} = \frac{-\dot{Q}_b - \dot{Q}_u}{\omega}, \tag{13}$$

$$\dot{Q}_b = h\sum_{i=h,p,l} A_{bi}(T_b - T_{wi}), \tag{14}$$

$$\dot{Q}_u = h\sum_{i=h,p,l} A_{ui}(T_u - T_{wi}), \tag{15}$$

wherein A_{bi} and A_{ui} are the areas of burnt and unburned gases in contact with each combustion chamber component at temperature T_{wi}, and subscripts h, p, and l refer to cylinder head, piston crown, and liner, respectively. The instantaneous heat transfer coefficient (h) adopted from Woschni [7] is given by

$$h = 0.82b^{-0.2}\left(p \cdot 10^{-3} \cdot U\right)^{0.8} T^{-0.53}, \tag{16}$$

where

$$U = 6.18\,\text{cm} \quad \text{(for gas exchange process)}, \tag{17}$$

$$U = 2.28\,\text{cm} + 0.00324T\frac{\Delta p}{p_{\text{IVC}}}\frac{V}{V_{\text{IVC}}} \quad \text{(for other processes)}, \tag{18}$$

$$T = xT_b + (1-x)T_u, \tag{19}$$

$$A_{bi} = A_i x^{1/2}, \tag{20}$$

$$A_{ui} = A_i\left(1 - x^{1/2}\right), \tag{21}$$

and Δp is the instantaneous pressure difference between the firing engine and motoring engine at the same crank angle. The latter is estimated by using the isentropic relation $pV^{\gamma} = p_{\text{IVC}}V_{\text{IVC}}^{\gamma}$. The surface areas in contact with hot gases can be expressed by

$$A_h = \frac{\pi b^2}{2} \quad \text{(hemispheric cylinder head)},$$

$$A_p = \frac{\pi b^2}{4} \quad \text{(flat piston crown)}, \tag{22}$$

$$A_l = \frac{4V(\theta)}{b} \quad \text{(liner surface area exposed to gases)}.$$

The cylinder volume at any crank angle is given by

$$V(\theta) = V_c\left\{1 + \frac{r-1}{2}\left\{1 - \cos\theta + \frac{1}{\varepsilon}\left[1 - \left(1 - \varepsilon^2\sin^2\theta\right)^{1/2}\right]\right\}\right\}. \tag{23}$$

Equations (20) and (21) assume that the fraction of cylinder area exposed to burnt gas is proportional to the square root of the burnt mass fraction which reflects the fact that burnt gas occupies a larger volume fraction than the unburned gas [16].

4.5. Blowby Energy Loss. The enthalpy loss due to blowby is expressed as

$$h_1 = (1 - x^2)h_u + x^2 h_b, \tag{24}$$

where h_u and h_b is unburned gases enthalpy and burned are one, which implicitly indicates that more leaking is due to the unburned gas compared with the burnt gas in the early stage of combustion.

4.6. Governing Equations. Differentiating the specific volume (6) with respect to crank angle and incorporating equation (8) yields

$$\begin{aligned}\frac{1}{m}\frac{dV}{d\theta} - \frac{VC_b}{m\omega},\\ = x\frac{\nu_b}{T_b}\frac{\partial \ln \nu_b}{\partial \ln T_b}\frac{dT_b}{d\theta} + (1-x)\frac{\nu_u}{T_u}\frac{\partial \ln \nu_u}{\partial \ln T_u}\frac{dT_u}{d\theta}\\ + \left[x\frac{\nu_b}{p}\frac{\partial \ln \nu_b}{\partial \ln p} + (1-x)\frac{\nu_u}{p}\frac{\partial \ln \nu_u}{\partial \ln p}\right]\frac{dp}{d\theta},\\ + (\nu_b - \nu_u)\frac{dx}{d\theta},\end{aligned} \tag{25}$$

where the blowby coefficient is $C_b = \dot{m}_1/m$ and m is the leakage due to blowby.

Expressing the heat loss of burnt and unburned gases as a function of the rate of change of specific entropy gives

$$\begin{aligned}-\dot{Q}_b &= m\omega x T_b \frac{ds_b}{d\theta},\\ -\dot{Q}_u &= m\omega(1-x)T_u\frac{ds_u}{d\theta},\end{aligned} \tag{26}$$

where

$$\begin{aligned}\frac{ds_b}{d\theta} &= \left(\frac{c_{pb}}{T_b}\right)\frac{dT_b}{d\theta} - \frac{\nu_b}{T_b}\frac{\partial \ln \nu_b}{\partial \ln T_b}\frac{dp}{d\theta},\\ \frac{ds_u}{d\theta} &= \left(\frac{c_{pu}}{T_u}\right)\frac{dT_u}{d\theta} - \frac{\nu_u}{T_u}\frac{\partial \ln \nu_u}{\partial \ln T_u}\frac{dp}{d\theta}.\end{aligned} \tag{27}$$

Combining equations (14)-(15), (20)-(21), (26), and (27), $ds_b/d\theta$ and $ds_u/d\theta$ terms are eliminated. Hence,

$$\begin{aligned}c_{pb}\frac{dT_b}{d\theta} - \nu_b\frac{\partial \ln \nu_b}{\partial \ln T_b}\frac{dp}{d\theta} &= \frac{-h\sum_{i=h,p,l}A_{bi}(T_b - T_{wi})}{m\omega x},\\ c_{pu}\frac{dT_u}{d\theta} - \nu_u\frac{\partial \ln \nu_u}{\partial \ln T_u}\frac{dp}{d\theta} &= \frac{-h\sum_{i=h,p,l}A_{ui}(T_u - T_{wi})}{m\omega(1-x)}.\end{aligned} \tag{28}$$

In addition to (24) and (28), differentiating equations (12)–(23) and incorporating these with (3), (5)-(6), (8), (11), and (13) into the energy equation (4), the following set of equations is obtained after substantial simplification:

$$\begin{aligned}\frac{dp}{d\theta} &= \frac{A+B+C}{D+E},\\ \frac{dT_b}{d\theta} &= \frac{-h\sum_{i=h,p,l}A_{bi}(T_b - T_{wi})}{m\omega x c_{pb}} + \frac{\nu_b}{c_{pb}}\frac{\partial \ln \nu_b}{\partial \ln T_b}\frac{dp}{d\theta}\\ &\quad + \frac{h_u - h_b}{xc_{pb}}\left[\frac{dx}{d\theta} + (x - x^2)\frac{C_b}{\omega}\right],\\ \frac{dT_u}{d\theta} &= \frac{-h\sum_{i=h,p,l}A_{ui}(T_u - T_{wi})}{m\omega c_{pu}(1-x)} + \frac{\nu_u}{c_{pu}}\frac{\partial \ln \nu_u}{\partial \ln T_u}\frac{dp}{d\theta},\end{aligned} \tag{29}$$

where

$$A = \frac{1}{m}\left(\frac{dV}{d\theta} + \frac{VC_b}{\omega}\right),$$

$$B = \frac{h}{\omega m}\left[\frac{\nu_b}{c_{pb}}\frac{\partial \ln \nu_b}{\partial \ln T_b}\frac{\sum_{i=h,p,l} A_{bi}(T_b - T_{wi})}{T_b} + \frac{\nu_u}{c_{pu}}\frac{\partial \ln \nu_u}{\partial \ln T_u}\frac{\sum_{i=h,p,l} A_{bi}(T_u - T_{wi})}{T_u}\right],$$

$$C = -(\nu_b - \nu_u)\frac{dx}{d\theta} - \nu_b \frac{\partial \ln \nu_b}{\partial \ln T_b}\frac{h_u - h_b}{c_{pb}T_b}\left[\frac{dx}{d\theta} - \frac{(x - x^2)C_b}{\omega}\right] \quad (30)$$

$$D = x\left[\frac{\nu_b^2}{c_{pb}T_b}\left(\frac{\partial \ln \nu_b}{\partial \ln T_b}\right)^2 + \frac{\nu_b}{p}\frac{\partial \ln \nu_b}{\partial \ln p}\right],$$

$$E = (1 - x)\left[\frac{\nu_u^2}{c_{pu}T_u}\left(\frac{\partial \ln \nu_u}{\partial \ln T_u}\right)^2 + \frac{\nu_u}{p}\frac{\partial \ln \nu_u}{\partial \ln p}\right]$$

are functions of θ, p, T_b, and T_u and their numerical integration can be obtained by using a fifth-order Runge-Kutta method.

The equations of the model exposed in this section are solved numerically using a marching technique with a time step size of 1 degree crank angle. Before the start of calculations, the design characteristics of the engine in hand are provided, as well as the operating data at the start of the cycle. The corresponding program is written in MATLAB programming language and executed on a Pentium-IV personal computer.

5. Results and Discussion

A comparison is made in this section between the measured values derived from the experimental investigation and the ones calculated by the model, so that the model could be tested performance-wise. Figure 3 shows the power-ignition timing diagram, while Figure 4 shows the torque-ignition timing diagram of the engine at a speed of 3400 rpm under different ignition timing conditions. 3400 rpm is chosen because it is in this speed that maximum torque for this engine is obtained.

The results show that power tends to increase with spark advance between 17 and 35°CA BTDC. It is expected that power should increase with spark advance to a point and then drop off. Best performance will be achieved when the greatest portion of the combustion takes place near top dead center. If the spark is not advanced enough, the piston will already be moving down when much of the combustion takes place. In this case, we lose the ability to expand this portion of the gas through the full range, decreasing performance. If ignition is too advanced, too much of the gas will burn while the piston is still rising. As a result, the work that must be done to compress this gas will decrease the net work produced. These competing effects cause a maximum in the power as a function of spark advance.

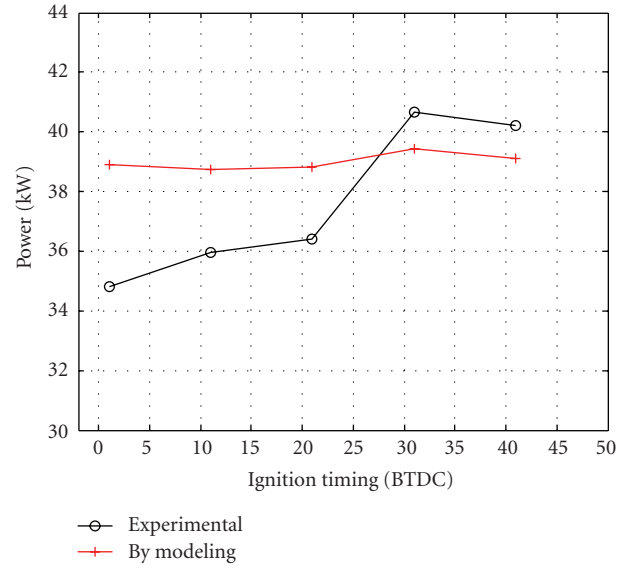

Figure 3: Comparison of predicted engine power with experimental data under varying ignition timing conditions at 3400 rpm.

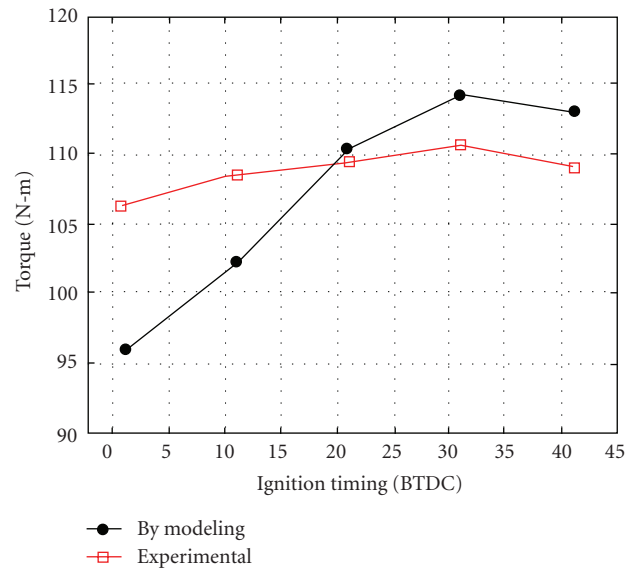

Figure 4: Comparison of predicted engine torque with experimental data under varying ignition timing conditions at 3400 rpm.

As is evident in Figure 4, the torque increases with increasing ignition advance. This is due to increasing pressure in the compression stroke, and consequently more net work is produced. It is necessary to mention that by further increase in spark advance, torque will not rise largely due to in-cylinder peak pressure during compression period and a decrease of pressure in expansion stroke. For this reason, determining the optimum ignition timing is one of the most important characteristics for an SI engine.

The difference between the simulated and experimental results can be noticed. These errors can be attributed to the frictional processes between engine components which are

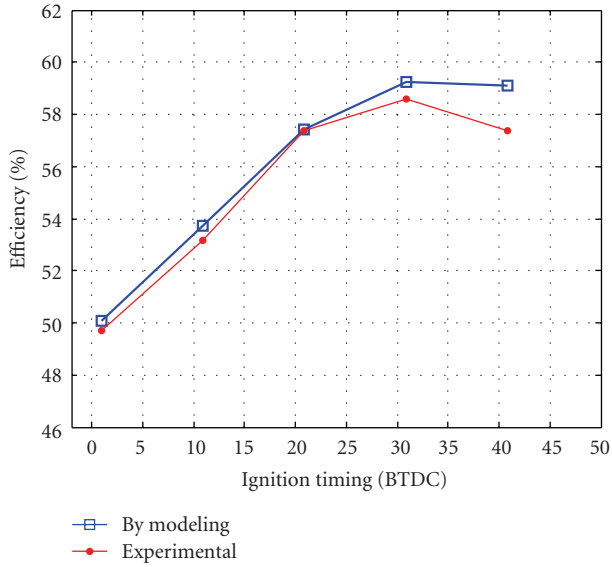

Figure 5: Comparison of predicted thermal efficiency with experimental data under varying ignition timing conditions at 3400 rpm.

Table 2: Comparison of predicted in-cylinder peak pressure under different ignition timing conditions.

Ignition timing (CA degree)	Peak pressure (Kpa)
−10	1855
1	2441
11	3239
21	4213
31	5470
41	6567

not considered in modeling. There are three types of friction that cause a waste of power in the internal combustion engines: (1) the mechanical friction between the internal moving parts such as piston and ring, (2) the pumping work which is the net work done during the intake and exhaust stroke, and (3) the accessory work. It means that these components gain their power from the engine, and therefore the net work decreases.

Predicted power is in good agreement with experimental data with the error of 2.97 percent, while the error of torque prediction is 3.22 percent at 31°CA BTDC of ignition timing. Both errors are generally acceptable for an engineering application.

Figure 5 presents the predicted results of thermal efficiency in comparison with experimental data. Thermal efficiency is work-out divided by energy-in. It can be seen that the net work increases with rising ignition advance to a point and then reduces slightly. This is due to increasing friction at high values of ignition advance and therefore reducing net work. According to Figure 6, the highest amount of the net work occurs at 31°CA BTDC.

Table 2 shows predicted in-cylinder peak pressure under varying ignition timing conditions. The results show that the peak pressure increases with increasing the ignition timing.

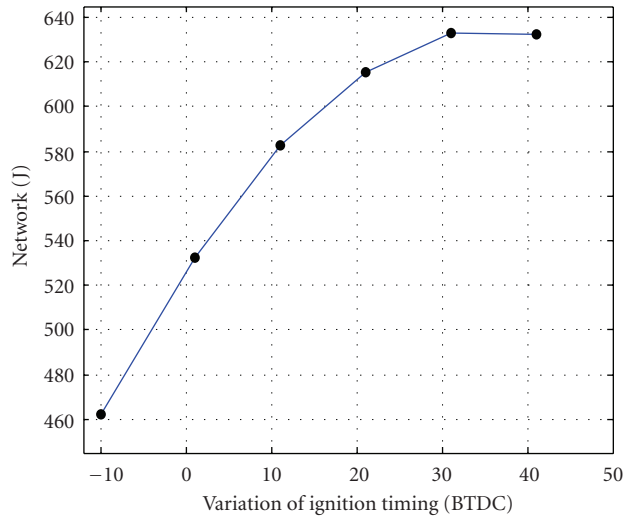

Figure 6: Predicted net work versus ignition timing.

But an increase in pressure does not certainly mean that thermal efficiency rises because if spark happens too early before top dead center, part of pressure exerts before piston reaches to top dead center and, consequently, the thermal efficiency decreases. Figure 6 also shows net work under varying ignition timing conditions. As Figure 6 shows, net work before and after 31 degree is reduced and maximum net work is at 31 degree.

Figure 7 shows the $p - V$ diagram, while Figure 8 shows $p - \theta$ diagram of the engine at a speed of 3400 rpm under varying ignition timing conditions. The results show that peak pressure increases with increasing ignition advance. It is known that the bigger the area of $p - V$ diagram, the more work produced. If the ignition is advanced, the combustion starts from the end of the compression stroke and finishes in the expansion stroke at the beginning of the top dead center. The combustion changes air-fuel mixture into combustion products and increases the in-cylinder temperature to high values. This phenomenon increases in-cylinder pressure to its maximum value in the engine cycle. Nevertheless, the maximum amount of the thermal efficiency and the net work cannot be concluded from the maximum pressure and temperature. Therefore, to determine the most efficient ignition timing, the least heat loss during the expansion stroke and also frictional losses should be considered. In this case, according to Figures 5 and 6, the optimum ignition timing is 31°CA BTDC due to the best net work and thermal efficiency.

Figure 9 plots the heat release diagram versus the crank angle under varying ignition timing conditions. The characteristic features of the heat release curve are an initial small slope reign beginning with spark ignition, followed by a region of rapid growth, and then a more gradual decay. During the combustion process, the heat loss decreases the maximum actual temperature and pressure in comparison with the condition of neglecting heat transfer. Therefore, the expansion stroke initiates at lower pressure and consequently the net work deceases. By continuing the heat transfer during

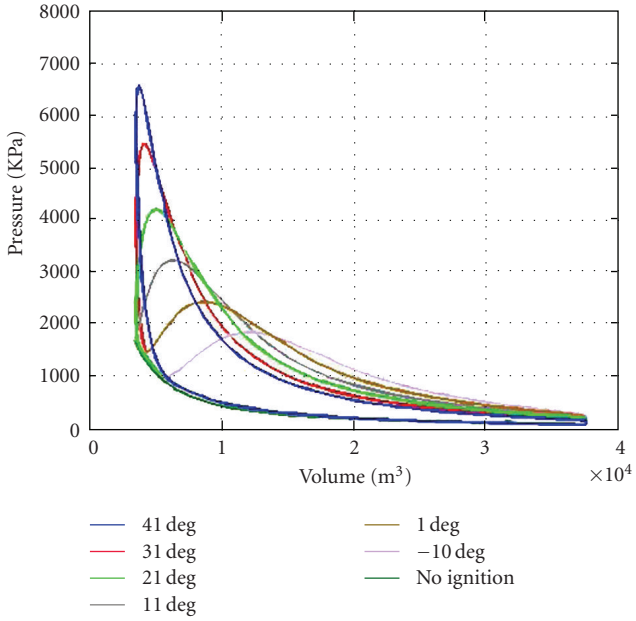

Figure 7: Comparison of predicted $p - V$ diagram under varying ignition timing conditions.

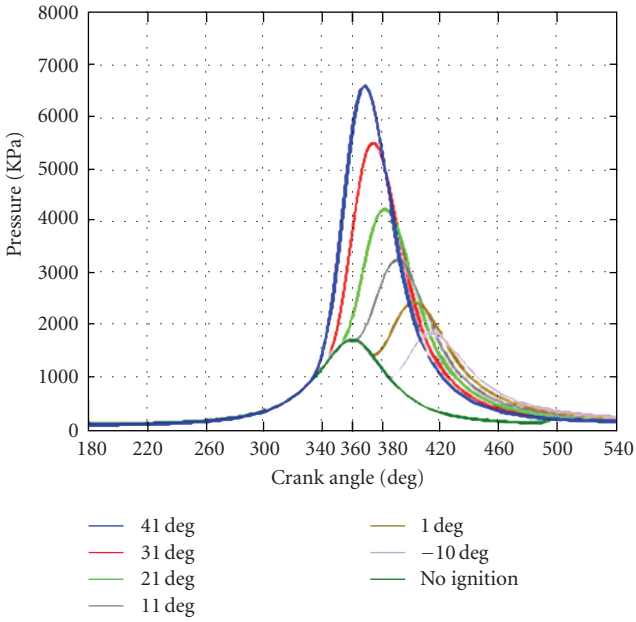

Figure 8: Comparison of predicted $p - \theta$ diagram under varying ignition timing conditions.

the expansion stroke, the temperature and pressure become smaller than those calculated by the isentropic expansion; consequently, the thermal efficiency decreases.

6. Conclusion

In the present work, the performance of a commercial SI engine under different ignition timing conditions was analyzed. This is in order to postulate the ignition timing for maximizing engine performance in terms of power, torque, thermal efficiency, and so forth. The following conclusions have been drawn.

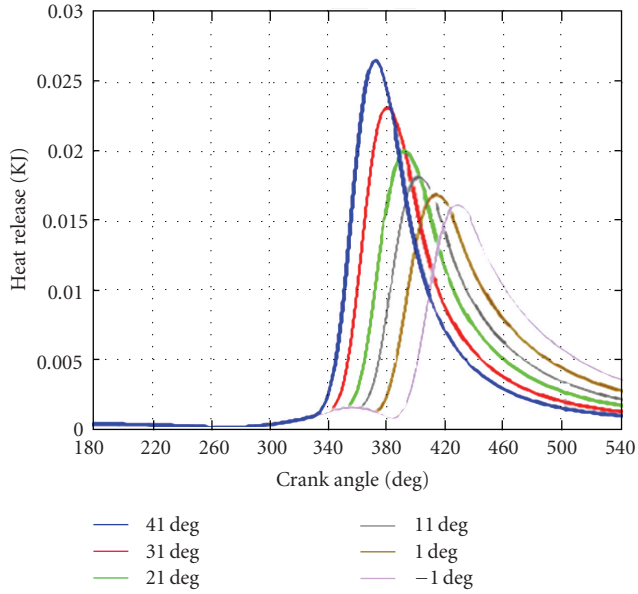

Figure 9: Comparison of predicted heat release crank angle under varying ignition timing conditions.

(1) If ignition timing does not become advance enough, most of the combustion occurs when the piston is moving down and, in this case, the power and the thermal efficiency decrease.

(2) If ignition timing gets too advance, most of the air-fuel mixture burns before the piston rises. Additionally, the period of the time of heat loss becomes larger, then the net work and the thermal efficiency decrease.

(3) By raising ignition advance, however, an increase in temperature and pressure in cylinder happens but the power and the thermal efficiency decrease due to higher friction loss and other losses in the engine.

(4) The performance of an SI engine highly depends on ignition timing, and its optimum value should be determined for each SI engine. For this engine, the maximum thermal efficiency and net work are obtained at 31°CA BTDC.

Nomenclature

A: Area exposed to hear transfer
ATDC: After top dead center
b: Cylinder bore
BTDC: Before top dead center
CA: Crank angle
cm: Piston mean speed
c_p: Specific heat at constant pressure
C_b: Blowby coefficient
E: Total energy

h: Specific enthalpy
l: Connecting rod length
m: Mass
n: Number
p: Pressure
Q: Heat transfer
r: Compression ratio
s: Specific entropy
S: Stroke length
T: Temperature
u: Specific internal energy
U: Internal energy
v: Specific volume
V: Volume
W: Work done
x: Burnt mass fraction
ε: $=S/2l$
γ: Ratio of specific heat
θ: Crank angle
θ_b: Combustion duration
θ_{ig}: Ignition timing
ω: Angular velocity.

Subscripts

b: Burnt gas
EVO: Exhaust valve opened
i: Intake
IVC: Intake valve closure
j: Component index
l: Blowby
u: Unburned gas
w: Wall.

Acknowledgments

This work has, in part, been supported by the Iran Khodro Education Center. This paper was recommended for publication in revised form by an associate Editor.

References

[1] S. H. Chan and J. Zhu, "Modelling of engine in-cylinder thermodynamics under high values of ignition retard," *International Journal of Thermal Sciences*, vol. 40, no. 1, pp. 94–103, 2001.

[2] S. Soylu and J. Van Gerpen, "Development of empirically based burning rate sub-models for a natural gas engine," *Energy Conversion and Management*, vol. 45, no. 4, pp. 467–481, 2004.

[3] R. B. Krieger and G. L. Borman, "The computation of apparent heat release for internal combustion engines," ASME paper no: 66-WA/DGP-4, 1966.

[4] P. N. Blumberg and J. T. Kummer, "Prediction of NO formation in spark ignited engines—an analysis of methods of control," *Combustion Science and Technology*, vol. 4, pp. 73–95, 1971.

[5] J. B. Heywood, *Internal Combustion Engines Fundamentals*, McGraw-Hill, New York, NY, USA, 1988.

[6] J. Abraham, F. V. Bracco, and R. D. Reitz, "Comparisons of computed and measured premixed charge engine combustion," *Combustion and Flame*, vol. 60, no. 3, pp. 309–322, 1985.

[7] A. Amsden, *A Block Structured KIVA Program for Engines with Vertical and Canted Valves*, National Laboratory, Los Alamos, NM, USA, 1999.

[8] S. Kong, N. Ayoub, and R. D. Reitz, "Modeling combustion in compression ignition homogeneous charge engines," in *Proceedings of the SAE International Congress and Exposition*, pp. 1–16, 1992, Technical Paper paper no. 920512.

[9] S. C. Kong and R. D. Reitz, "Use of detailed chemical kinetics to study HCCI engine combustion with consideration of turbulent mixing effects," *Journal of Engineering for Gas Turbines and Power*, vol. 124, no. 3, pp. 702–707, 2002.

[10] S. Soylu, *Autoignition modeling of natural gas for engine modeling programs: an experimental and modeling study*, Ph.D. thesis, Iowa State University, 2001.

[11] I. M. Khan, G. Greeves, and D. M. Probert, "Prediction of soot and nitric oxide concentrations in diesel engine exhaust. Air pollution control in transport engines," *Institution of Mechanical Engineers, Part C*, vol. 142, no. 71, pp. 205–217, 1971.

[12] N. D. Whitehouse and B. K. Sareen, "Prediction of heat release in a quiescent chamber Diesel engine allowing for fuel/air mixing," SAE paper no. 740084, 1974.

[13] C. D. Rakopoulos, G. N. Taklis, and E. I. Tzanos, "Analysis of combustion chamber insulation effects on the performance and exhaust emissions of a DI diesel engine using a multi-zone model," *Heat Recovery Systems and CHP*, vol. 15, no. 7, pp. 691–706, 1995.

[14] C. D. Rakopoulos and D. T. Hountalas, "Development and validation of a 3-D multi-zone combustion model for the prediction of DI diesel engines performance and pollutants emissions," *Journal of Engines*, vol. 107, p. 1413, 1998.

[15] C. D. Rakopoulos and D. T. Hountalas, "Development of a new 3-D multi-zone combustion model for indirect injection diesel engines with a swirl type prechamber," *Journal of Engines*, vol. 109, p. 718, 2000.

[16] C. R. Ferguson and A. T. Krikpatrick, *Internal Combustion Engines—Applied Thermosciences*, John Wiley & Sons, New York, NY, USA, 2001.

[17] C. Olikara and G. L. Borman, "A computer program for calculating properties of equilibrium combustion products with some applications on IC engines," SAE paper no. 750468, 1975.

[18] J. B. Heywood, *Engine Combustion Modeling—An Overview from Combustion Modeling in Reciprocating Engines*, Plenum Press, 1980.